RECONSTRUCTION OF PREVAILING SURFACE WIND REGIMES ON MARS USING ECMWF REANALYSIS DATA, REMOTE SENSING IMAGES OF AEOLIAN LANDFORMS, AND A CONVOLUTIONAL NEURAL NETWORK. J. Kong[1,2,3], J. K. Lundquist[1,4,5], and P. O. Hayne[2,6] [1]Department of Atmospheric and Oceanic Sciences, [2]Department of Astrophysical and Planetary Sciences, and [3]Department of Geography, University of Colorado Boulder, Boulder, CO 80309, USA; [4]Renewable and Sustainable Energy Institute, Boulder, CO 80309, USA; [5]National Renewable Energy Laboratory, Golden, CO 80401, USA. [6]Laboratory for Atmospheric and Space Physics, Boulder, CO 80303, USA.

Introduction: Previous studies have suggested the feasibility of using machine learning techniques to develop and achieve automated detection, recognition, and mapping of different landform features on a planetary surface, such as barchan dunes, transverse ridges, and slope streaks [1]. Furthermore, some researchers have reported the practical application of Convolutional Neural Networks (CNNs) to classify Mars landforms [2]. Moreover, reconstruction of wind patterns over Mars has been previously practiced by mapping the large ripples and sand dunes on Mars [3], applying GIS techniques with digital terrain models (DTMs) [4], and manually tracing the waves and ripple migration directions on the remote sensing data [5]. However, relevant studies have yet to be found to combine machine learning techniques, remote sensing data of aeolian landforms, and available climate reanalysis to reconstruct the wind patterns on Mars.

In this study, we propose and practice a method that applies a CNN with the remote sensing data of aeolian landform features and prevailing surface wind data on Earth as a reference to train a machine learning model for reconstructing the winds on Mars. In the absence of in-situ wind direction data, we compare our obtained results against the prevailing surface winds derived from the GFDL/NASA Mars General Circulation Model (MGCM) [6] output for assessment regarding the performance, feasibility, and the outcome of this method, and obtain the best possible understanding.

Approach and Methods: MobileNet Version 2, a lightweight CNN architecture proposed by Google for balancing the demands for computational time and performance [7], was applied to train a machine learning model with the prevailing surface wind and the remote sensing data on Earth. For Earth, the prevailing surface wind data was derived from the 5-generation ECMWF atmospheric reanalysis (ERA5) of the global Earth climate [8]. The ERA5 variables of 10-m zonal (U10) and meridional (V10) surface winds, requested through the Climate Data Store (CDS) API [8], were used to calculate the wind speed and direction and were averaged for 20 years to recognize the prevailing surface winds at a 9-km spatial resolution. Multispectral remote sensing data of ~1600 sites with aeolian landforms selected from about 50 regions worldwide were then collected through the Google Earth Engine (GEE) API [9]. The acquired optical bands of remote sensing data (B2-B7) are blue, green, red, NIR, SWIR-1, and SWIR-2, all with a resolution of 30 m and an extent of 3×3 km, and with the center coordinates of the wind data as the reference for alignment and labeling. Before training, the remote sensing data were cleaned to remove all broken and problematic data.

The data were then randomly divided into 80% training, 10% validation, and 10% testing datasets. After the training process was completed, the trained model was applied to the testing dataset to observe the performance of the method. The trained model was then applied to six remote sensing data from Mars, and the results were compared against the Ensemble Mars Atmosphere Reanalysis System (EMARS) Version 1.0 [10]. EMARS is a collection of GFDL/NASA MGCM model output and a climate reanalysis consisting of an extended, retrospective analysis sequence that contains hourly gridded atmospheric variables for Mars, spanning Mars Year (MY) 24 through 33, where we used the data for the MY 24 to 26.

Figure 1. The best six results of applying the trained model on the testing dataset. Yellow arrows show the reconstructed wind directions.

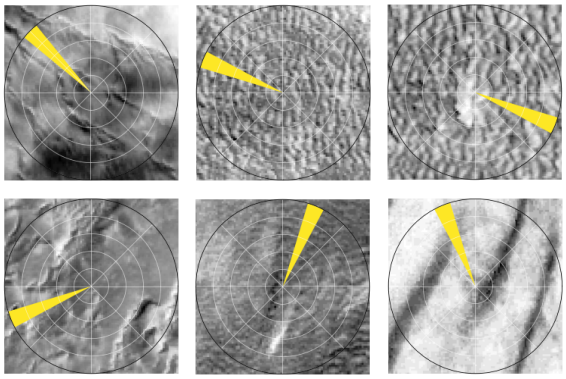

Figure 2. Histograms of the difference between the reconstructed and ERA5-derived wind speed ($m \cdot s^{-1}$) and the reconstructed and ERA5-derived direction (degrees) on testing dataset. The NRMSEs are 0.106 (wind speed) and 0.117 (wind direction).

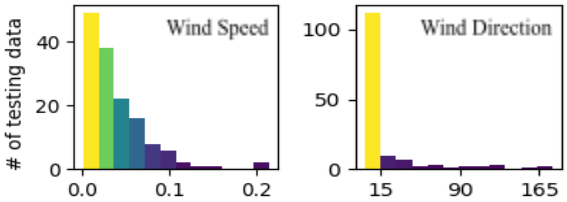

Results: Figure 1 shows the six best accuracy results obtained from the test dataset by applying the trained model, compared to the ERA5-derived data. Figure 2 shows an overview of all results based on the testing dataset. The histograms show that the reconstructed wind directions are less than 15 degrees closer to the ERA5-derived prevailing wind directions for most test results and that the reconstructed wind speeds are close to the ERA5-derived wind speeds. Figure 3 shows the plot of training loss versus the validation loss for evaluating the model performance, where the training loss indicates how well the model fits the training data. In contrast, the validation loss suggests how well the model fits the validation data. The plot shows that the training loss and validation loss both decrease and stabilize at a specific point, and both values end up roughly the same, suggesting that the model was trained pretty well.

Since we think that using our trained model for wind speed prediction may not be reliable on Mars, which has very different atmospheric properties than Earth, the trained model was only applied to Mars remote sensing data for predicting the prevailing surface wind directions. Six remote sensing data were selected for the application, and the results shown are in Figure 4. The trained model doesn't work perfectly well on Mars but can infer the general orientation of the prevailing surface winds within 60 degrees to the EMARS-derived wind directions.

Figure 3. Model performance: comparison of training loss with validation loss during the training process.

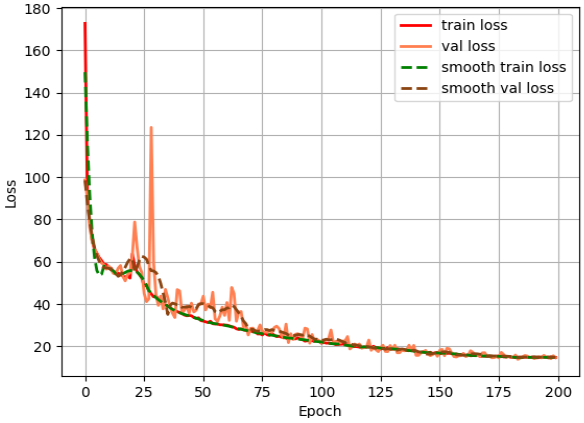

Figure 4. Mars remote sensing data, taken by the High Resolution Imaging Experiment camera (HIRISE) [11], the spatial extents vary from ~3 to ~8 km, and the resolutions were downsampled to 30 m.

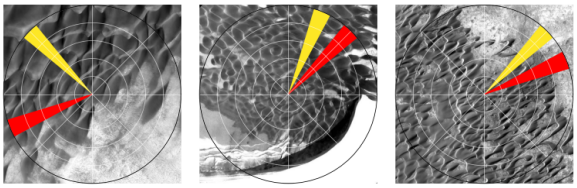

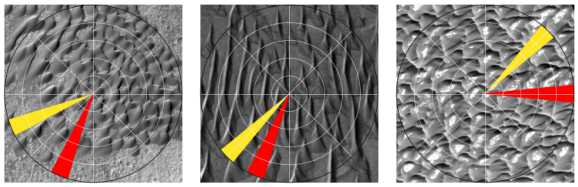

Limitations and Improvable Aspects: Limitations of this approach include the fact that we didn't consider the artifacts on some Earth remote sensing data and that some places may not have aeolian landforms, which may affect the results of wind reconstruction. We suggest adding a dune classification model for further cleaning the remote sensing data before training. We also didn't do any data augmentation, but doing this augmentation would significantly increase the amount of available data for training but would also require a lot more computational time and power. In addition, for application on Mars, we converted the HiRISE data to the same resolutions as the Landsat-8 (30m), which may lead to some inaccuracies in the wind reconstruction results. So we also suggest more appropriate practices in considering these aspects for the future.

Conclusion: We proposed and implemented an applied deep learning approach to train a model with remote sensing data of aeolian landforms and wind data on Earth as a reference to reconstruct the winds of Mars. The reconstructed wind using our trained model may be partially consistent with sand dune and ripple morphology on Mars. It may not represent current or paleo-wind regimes but can add a reference or a 'snapshot' of the potential wind flow patterns of regions with dunes on Mars. And we can suspect that this inconsistency may result from the historical climate change on Mars and, thus, a change in surface circulations. However, more work needs to be done, and verifications with in-situ observations are much desired in the future.

References: [1] Hugenholtz, H. C. et al. (2011) *Earth Sci. Rev., 111,* 319-334. [2] Palafox, L. F. (2017) *Comput. Geosci., 101,* 48-56. [3] Zimbelman, J. R. (2017) *LPS XLVIII,* Abstract #2252. [4] Johnson, M. B. (2015) *IPDW IV,* Abstract #8015. [5] Hood, D. R. et al. (2021). *Front. Earth Sci., 9*, 702828. [6] Newman, C. E. (2002) *J. Geophys. Res., 107,* 6-1-6-18. [7] Sandler, M. (2018) *IEEE CVPR.,* 4510-4520. [8] Hersbach, H. (2020) *Q. J. R. Meteorol. Soc., 146,* 1999-2049. [9] Gorelick, Noel. et al (2017). *Remote Sens. Environ., 202,* 18-27. [10] Greybush, S. J (2019). *Geosci. Data J., 6,* 137-150. [11] McEwen, A. S. (2007) *J. Geophys. Res., 112,* E5.